MIT Libraries | DSpace@MIT

MIT Open Access Articles

Contrasting Effects of Vasculogenic Induction Upon Biaxial Bioreactor Stimulation of Mesenchymal Stem Cells and Endothelial Progenitor Cells Cocultures in Three-Dimensional Scaffolds under in Vitro and in Vivo Paradigms for Vascularized Bone Tissue Engineering

Massachusetts Institute of Technology

Contrasting Effects of Vasculogenic Induction Upon Biaxial Bioreactor Stimulation of Mesenchymal Stem Cells and Endothelial Progenitor Cells Cocultures in Three-Dimensional Scaffolds Under *In Vitro* and *In Vivo* Paradigms for Vascularized Bone Tissue Engineering

Yuchun Liu, BEng,[1–3] Swee-Hin Teoh, PhD,[3] Mark S.K. Chong, PhD,[1] Chen-Hua Yeow, PhD,[4,5]
Roger D. Kamm, PhD,[6,7] Mahesh Choolani, FRCOG, PhD,[1] and Jerry K.Y. Chan, MRCOG, PhD[1,8,9]

Clinical translation of bone tissue engineering approaches for fracture repair has been hampered by inadequate vascularization required for maintaining cell survival, skeletal regeneration, and remodeling. The potential of vasculature formation within tissue-engineered grafts depends on various factors, including an appropriate choice of scaffold and its microarchitectural design for the support of tissue ingrowth and vessel infiltration, vasculogenic potential of cell types and mechanostimulation on cells to enhance cytokine expression. Here, we demonstrated the effect of biomechanical stimulation on vasculogenic and bone-forming capacity of umbilical-cord-blood endothelial progenitor cells (UCB-EPC) and human fetal bone marrow-derived mesenchymal stem cell (hfMSC) seeded within macroporous scaffolds and cocultured dynamically in a biaxial bioreactor. Dynamically cultured EPC/hfMSC constructs generated greater mineralization and calcium deposition consistently over 14 days of culture (1.7-fold on day 14; $p < 0.05$). However, *in vitro* vessel formation was not observed as compared to an extensive EPC-vessel network formed under static culture on day 7. Subsequent subcutaneous implantations in NOD/SCID mice showed 1.4-fold higher human:mouse cell chimerism ($p < 0.001$), with a more even cellular distribution throughout the dynamically cultured scaffolds. In addition, there was earlier evidence of vessel infiltration into the scaffold and a trend toward increased ectopic bone formation, suggesting improved efficacy and cellular survival through early vascularization upon biomechanical stimulation. The integrative use of bioreactor culture systems with macroporous scaffolds and cocultured osteogenic and vasculogenic cells promotes maturation of EPC/hfMSC-scaffold grafts necessary for vascularized bone tissue engineering applications.

Introduction

BONE IS A HIGHLY vascularized organ and reliant on the supply of blood vessels for the maintenance of cell survival during skeletal repair and growth.[1] Current bone tissue-engineered (BTE) constructs suffer a lack of sufficient vascularity within larger grafts, resulting in cellular necrosis especially at the core, leading to the eventual failure of the BTE graft over time.[2] To date, few pilot clinical studies[3–5] have reported evident success in the cell-based BTE approach for the treatment of large bone defects, with Marcacci's team showing vascularization of the grafted region after 6.5 years postsurgery.[6] However, most studies still lack clear data demonstrating early vasculature development

[1]Experimental Fetal Medicine Group, Department of Obstetrics and Gynaecology, Yong Loo Lin School of Medicine, National University of Singapore, Singapore.
[2]BIOMAT, Department of Mechanical Engineering, Faculty of Engineering, National University of Singapore, Singapore.
[3]Division of Bioengineering, School of Chemical and Biomedical Engineering, Nanyang Technological University, Singapore.
[4]Department of Bioengineering, Faculty of Engineering, National University of Singapore, Singapore.
[5]Harvard School of Engineering and Applied Sciences, Harvard University, Cambridge, Massachusetts..
[6]Departments of Biological Engineering and Mechanical Engineering, Massachusetts Institute of Technology, Cambridge, Massachusetts.
[7]Singapore-MIT Alliance for Research & Technology, Singapore.
[8]Department of Reproductive Medicine, KK Women's and Children's Hospital, Singapore.
[9]Cancer and Stem Cell Biology Program, Duke-NUS Graduate Medical School, Singapore.

within the graft necessary for graft survival, and eventual integration and long-term remodeling. Challenges relating to achieving adequate vascularization within synthetic bone grafts remain a major concern,[7] hence, limiting the introduction of BTE into the clinical setting.

To approach this clinical challenge, several strategies have been studied, such as the use of porous scaffolds, growth factors, and highly potent stem cells with vasculogenic potential.[8,9] Another approach rapidly gaining traction is in the generation of prevascularization, often through the use of both vasculogenic and osteogenic cell cocultures seeded within the scaffolds. While this strategy has achieved the formation of extensive prevascularized networks,[10–12] few have demonstrated enhanced bone formation,[13,14] which may be due to a lack of appropriate stimulus for rapid development of new blood vessels into these coculture grafts. This may be due to the inefficiencies of static culture conditions in generating such a graft. To date, only one group has reported the use of a dynamic environment for coculture systems in BTE, where dynamically cocultured scaffolds were compared to their monocultures rather than statically cultured cocultures.[15] Also, the effects of enhanced mass transport and biomechanical forces on cocultures of vasculogenic and osteogenic cell types have not been defined.

We have previously demonstrated the effects of efficient dynamic culture of human fetal bone marrow-derived mesenchymal stem cells (hfMSC) using a biaxial bioreactor, with improvements in cellular survival and osteogenic differentiation, and its efficacy for bone repair.[8,16,17] In this work, hfMSC and umbilical-cord-blood endothelial progenitor cells (UCB-EPC) have been chosen for their robust osteogenic[18] and angiogenic[19] potential, respectively. We hypothesized that the application of fluid shear stresses will enhance vasculogenesis of EPC and improve osteogenic differentiation of hfMSC in a coculture system supported by a three-dimensional (3D) honeycombed-like polycaprolactone tricalciumphosphate (PCL/TCP) scaffold. We envision that the utility of EPC/hfMSC stem cells in coculture, further stimulated by biomechanical forces using a biaxial bioreactor culture, will be an advantageous approach over other existing coculture systems.

Materials and Methods

Samples, animals, and ethics

Human tissue collection for research purposes was approved by the Domain Specific Review Board of National Healthcare Group (DSRB-D-06-154), in compliance with international guidelines regarding the use of fetal tissue for research as previously described.[8] In all cases, patients gave separate written consent for the use of the collected tissue. Fetal femurs were collected for isolation of hfMSC after clinically indicated termination of pregnancy. In this study, a sample derived from a 17^{+3} weeks^{+days} gestation was used. Human UCB samples from newborns were collected from normal full-term deliveries.

Male NOD SCID mice (6–8 weeks old) were acquired from the Animal Resources Centre. All procedures were approved by the Institutional Animal Care and Use Committee (IACUC) at the National University of Singapore, and procedures performed in AAALAC accredited animal facilities.

Isolation, culture, and characterization of hfMSC and EPC

hfMSC were isolated from bone marrow as previously described.[18] Briefly, single-cell suspensions were prepared by flushing the bone marrow cells from femurs using a 22-gauge needle, passed through a 70-μm cell strainer (BD Falcon) and plated on 10-cm plates (NUNC) at 10^6 cells/mL. Adherent spindle-shaped cells were recovered from the primary culture after 4 to 7 days. Nonadherent cells were removed with initial media changes every 2–3 days. At subconfluence, they were trypsinized and replated at 10^4 cells/cm^2. MSCs were cultured in the Dulbecco's modified Eagle's media-Glutamax (GIBCO) supplemented with 10% fetal bovine serum (FBS), 50 U/mL penicillin, and streptomycin (GIBCO), thereafter referred to as D10 media. Cells from passage 2–4 were characterized as previously described.[8,20]

UCB-derived EPC were obtained as previously described.[21] Briefly, blood was diluted and overlaid onto Ficoll-Paque PLUS (Amersham). Mononuclear cells from the buffy coat retrieved from UCB by low-density centrifugation were resuspended in endothelial growth media (EGM; Cambrex) supplemented with 10% FBS, thereafter referred to as EGM10, and then plated onto 100-mm tissue culture dishes coated with type I rat tail collagen (BD Biosciences) at 37°C, 5% CO_2 in a humidified incubator. Culture media was changed every 3 days subsequently. Typical cobblestone colonies appeared after 2 weeks, and were subcultured at subconfluence. Their endothelial differentiation on Matrigel and immunophenotypic characteristics were demonstrated by its expression of DiI acetylated low density lipoprotein (acLDL) uptake (Dako), CD31 (Millipore), the von Willebrand Factor (vWF) (Millipore), and VE Cadherin (Enzo Life Sciences) (Fig. 1).

Lentiviral transduction of EPC and hfMSC

The lentiviral vectors were produced as described previously.[20] Briefly, the transfer plasmids (pHIV-dTomato and pRRLSIN.cPPT.PGK-GFP.WPRE) were cotransfected with pHIV-Luciferase and pCMV.ΔR8.74 into HEK293T cells. The supernatant was collected at 48 and 72 h following transfection and concentrated by one round of ultracentrifugation at 50,000 g for 2 h, and the final pellet was dissolved in a small volume of 1% bovine serum albumin in phosphate-buffered saline (PBS) (1/100 of starting volume). The number of transducing units (TUs) of the vectors was determined by infecting 100,000 293T cells using serial dilution of the vector. The dilution resulting in < 30% GFP- or RFP-positive cells was used to calculate the number of TUs per mL. For transduction, cells were seeded at 0.5×10^4 cells/cm^2 in T-25 flasks, and exposed to lentivirus with 4 mg/mL polybrene at multiplicity of infection of 5. GFP-labeled EPC and RFP-labeled hfMSC at > 90% transduction efficiencies were used in the experiments.

Other media preparation

Bone media. Well-defined bone media (BM) was prepared using the D10 medium supplemented with bone inducing elements—10 mM β-glycerophosphate, 10^{-8} M Dexamethasone, and 0.2 mM Ascorbic acid (Sigma Aldrich).

Osteogenic assays

Calcium deposition was assayed as previously described.[8] Briefly, each sample well ($n = 3$) was incubated with 0.5 N
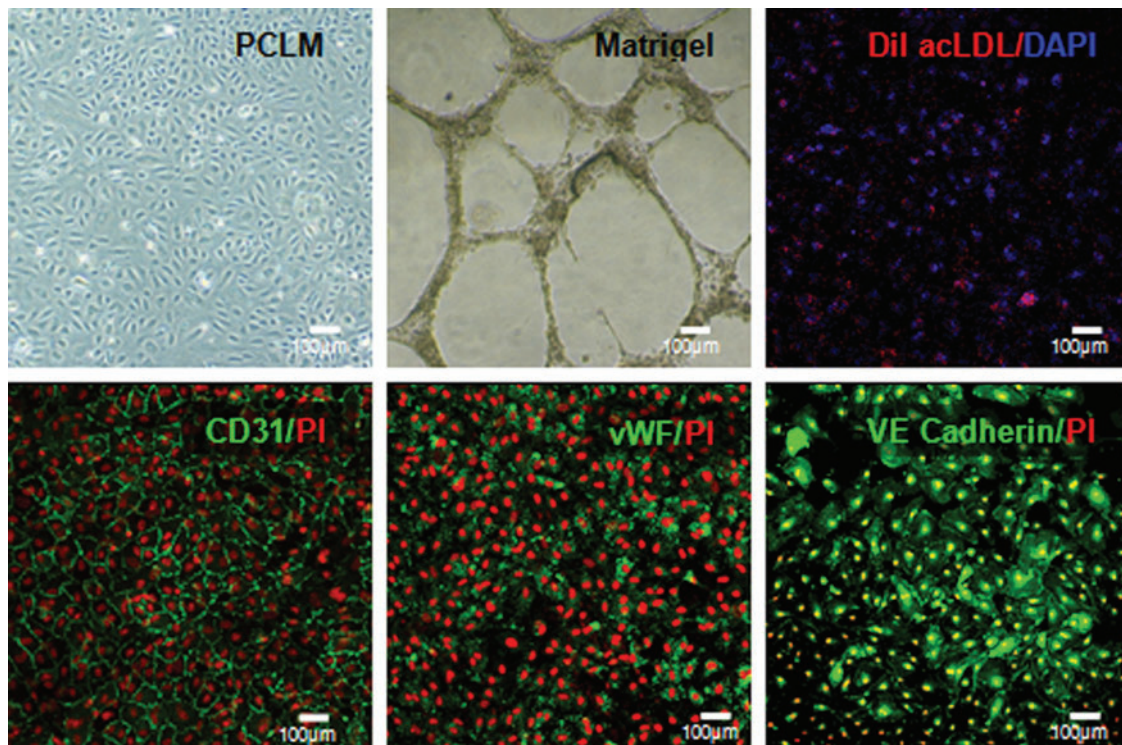
FIG. 1. Characterization of umbilical-cord-blood endothelial progenitor cells (UCB-EPC) using phase-contrast light microscopy (pCLM) showed the emergence of cobblestony colonies, which differentiated and formed tube-like networks on Matrigel. Immunophenotype of EPC were demonstrated by its expression of CD31, vWF, VE Cadherin, and acLDL uptake, with cell nuclei counterstained with propidium iodide (PI) and 4′,6-diamidino-2-phenylindole (DAPI) accordingly. Color images available online at www.liebertpub.com/tea

acetic acid overnight to dissolve calcium. A colorimetric calcium assay kit (BioAssay Systems) was used to quantitate the calcium content spectrophotometrically at 612 nm according to the manufacturer's instruction. Calcium from the PCL/TCP scaffolds was leached out from empty scaffolds and subtracted off from the measured calcium levels.

Alkaline phosphatase (ALP) was assayed as previously described.[8] Briefly, samples ($n = 3$) were gently rinsed twice with PBS, and incubated in 1 mg/mL of Collagenase Type 1 (Sigma Aldrich) dissolved in a 0.1% Trypsin (Invitrogen) solution and incubated at 37°C for 2 h to digest the extracellular matrix completely. After three cycles of freeze–thaw, the cell lysate solution was assayed for ALP activity using the SensoLyte™ pNPP Alkaline Phosphatase Assay Kit (AnaSpec) following the manufacturer's instruction.

The Von Kossa staining was performed as previously described.[8] Briefly, samples were gently rinsed twice with PBS, then fixed with 10% formalin for 1 h, followed by two washes with distilled water, and stained with freshly made 2% Silver nitrate (Sigma Aldrich) in distilled water (w/v) for 10 min in the dark and exposed to sunlight for 30 min.

Preparation of cellular–scaffold constructs

Scaffold fabrication and treatment. Macroporous PCL-TCP (80/20) scaffolds (Osteopore International) with a lay-down pattern of 0/60/120°, porosity of 70% were fabricated using a fused deposition modeling technique under the cGMP environment (ISO 13485) (Fig. 2A, B). Scaffolds were cut into 4X4X4mm dimensions and treated with 5 M NaOH for 3 h to enhance hydrophilicity, washed thoroughly with PBS thrice before disinfection by immersion in 100% ethanol overnight.

Cell loading and culture. Cells were suspended in Tisseel Fibrin Sealant (Baxter) before seeding into the porous scaffolds, keeping the EPC cell density constant at 3000 cells per mm³ of empty scaffold space in both study groups. EPC/hfMSC cocultures were used in a 1:1 ratio as optimized in our previous study.[22] The seeded cells were left to adhere to the scaffolds for 2 h under static conditions before transfer to sterile 24-well plates for static culture or a biaxial bioreactor culture for 14 days in BM culture.

Bioreactor setup

The bioreactor setup is as previously described in Zhang et al.[16,17] Briefly, the biaxial bioreactor consists of a spherical culture chamber in which the cellular scaffolds are anchored to the cap of the bioreactor by pins, a medium reservoir and a perfusion system, which connects the culture chamber and the medium reservoir. The spherical culture chamber is designed to rotate in two perpendicular axes (Y and Z, pink block arrows) simultaneously and perfused with media flow circulating between the culture chamber and the medium reservoir (Fig. 2C, D).

In vivo transplantation and assays

Under general anesthesia, acellular, and cellular–scaffold constructs were implanted into subcutaneous pockets generated at the dorsal surface of each immunodeficient mice,

FIG. 2. Microarchitectural design of polycaprolactone tricalcium phosphate (PCL/TCP) scaffolds and the design of the biaxial bioreactor setup. **(A)** Three-dimensional (3D) PCL/TCP scaffolds shown here **(B)** showing the honey-combed-like arrangement of polymeric material on scanning electron microscope (SEM). **(C, D)** The biaxial bioreactor with two rotational axes (indicated by pink block arrows), with scaffolds pinned and fixed in place while the bioreactor rotates, can be placed within an incubator. Color images available online at www.liebertpub.com/tea
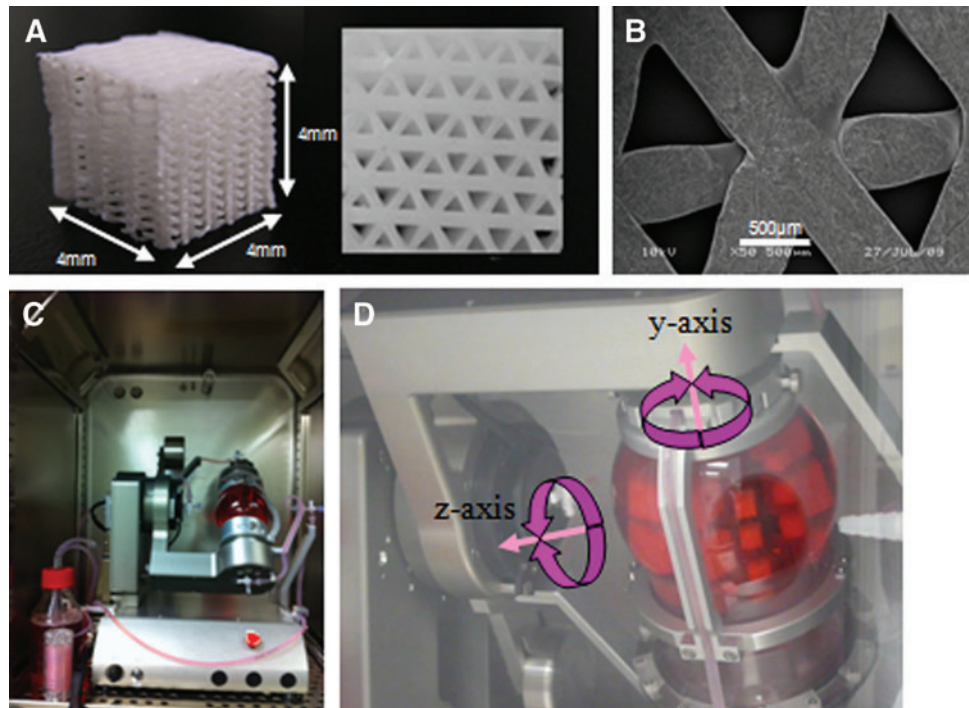
and the skin closed with 5-O Vicryl sutures. Scaffolds were harvested at weeks 4 and 8 for analysis.

Imaging

Phase-contrast light microscopy. Cellular morphology, adhesion, and extracellular matrix production were examined daily and imaged at fixed time intervals using an attached camera unit.

Confocal microscope. Cryosections of harvested cellular–scaffold constructs and 3D cultures were viewed and scanned under a confocal laser microscope using laser wavelengths of 405 nm (green), 594 nm (red) (Olympus, FV300 Fluoview). Image Analysis software Imaris (Bitplane) were used for the quantification Lamins A/C staining of 10 different regions of the cryosections as well as for image analysis.

Scanning electron microscope. Glutaldehyde-fixed scaffolds were then dehydrated, air-dried, and gold sputtered with the SCD 005 gold sputter machine (Bal-Tec) for 70 s at 30 mA under high vacuum before imaging on the scanning electron microscope (SEM) (JSM 5660; JEOL).

Microcomputed tomography. The harvested cellular–scaffold constructs were fixed in 10% formalin for 1 week before analysis of bone or vasculature network using the microcomputed tomography (Micro-CT) scanner (SMX-100CT X-ray CT Sys; Shimadzu). The scan settings were X-ray voltage = 45 kV, X-ray current = 100 μA, detector size = 9, scaling coefficient = 50, and voxel resolution = 0.008 mm. The scans were then reconstructed using VGStudioMax (Version 1.2; Volume Graphics) to create the 3D geometry and for quantitative histomorphometric analysis and calibrated against its background.

Vascularization assay

Micro-CT evaluation of vascularization was evaluated with the use of a blue vascular contrast, Microfil (MV-120; Flow Tech). Briefly, the mice were anesthetized, laid supine, and a midline incision extending across the thorax and abdomen was made. The left ventricle was cannulated and a perforation was made in the right atrial appendage before perfusion with heparinized saline. Upon complete exsanguination, 10 mL of the microfil solution diluted in the MV-diluent (1:1) along with the MV-curing agent (10% of total volume) was then perfused via a syringe. The mice were then stored at 4°C for 2 h for the silicon compound to polymerize before the scaffolds were harvested and fixed in 4% paraformaldehyde for a week before Micro-CT imaging.[8,23]

Histology

Cellular–scaffold constructs were placed on crushed dry ice for slow freezing and sectioned at 10 μm thickness transversely with a Cryostat (CM 3050S; Leica). Sections were stained with Masson's Trichrome (MT) to visualize tissue morphology and evidence of new bone formation. Capillary density was quantitated by evaluating the entire area of histological sections. Luminal structures perfused with red blood cells were identified as capillaries. The capillary density was calculated by dividing the total number of red blood cell-filled capillaries by the area of each section (vessels/mm^2).

Immunohistochemistry

Human mouse chimerism. Lamins A/C immunostaining was used to investigate chimerism of human cells in murine tissue. Cryosections from each sample were blocked with 5% normal goat serum for 1 h, and left to react with a monoclonal mouse anti-human Lamins A/C antibody (1:100; Vectorlabs)

overnight; sections were then incubated with goat anti-mouse secondary antibodies (1:100 Alexaflour 488; Invitrogen) for 1 h, and counterstained with propidium iodide. Images were visualized through confocal microscopy as above.

Osteopontin staining. The contribution of human cells to *in vivo* bone regeneration was delineated with human-specific osteopontin staining (1:100; Abcam) as previously described.[8]

Statistical analysis

Parametric data are presented as mean ± standard deviation and were analyzed by the *t*-test or analysis of variance.

$*p < 0.05$, $**p < 0.01$, $***p < 0.001$ indicate statistically significant differences between samples ($n = 3$).

Results

Characterization of UCB-EPC

UCB-EPC emerged as colonies with a cobblestone morphology, which differentiated and formed tube-like networks on Matrigel. EPC expressed endothelial markers, such as CD31, vWF, VE Cadherin, and scavenged acLDL (Fig. 1). hfMSC had a spindle morphology, which were negative for hemopoietic and endothelial markers (CD14,
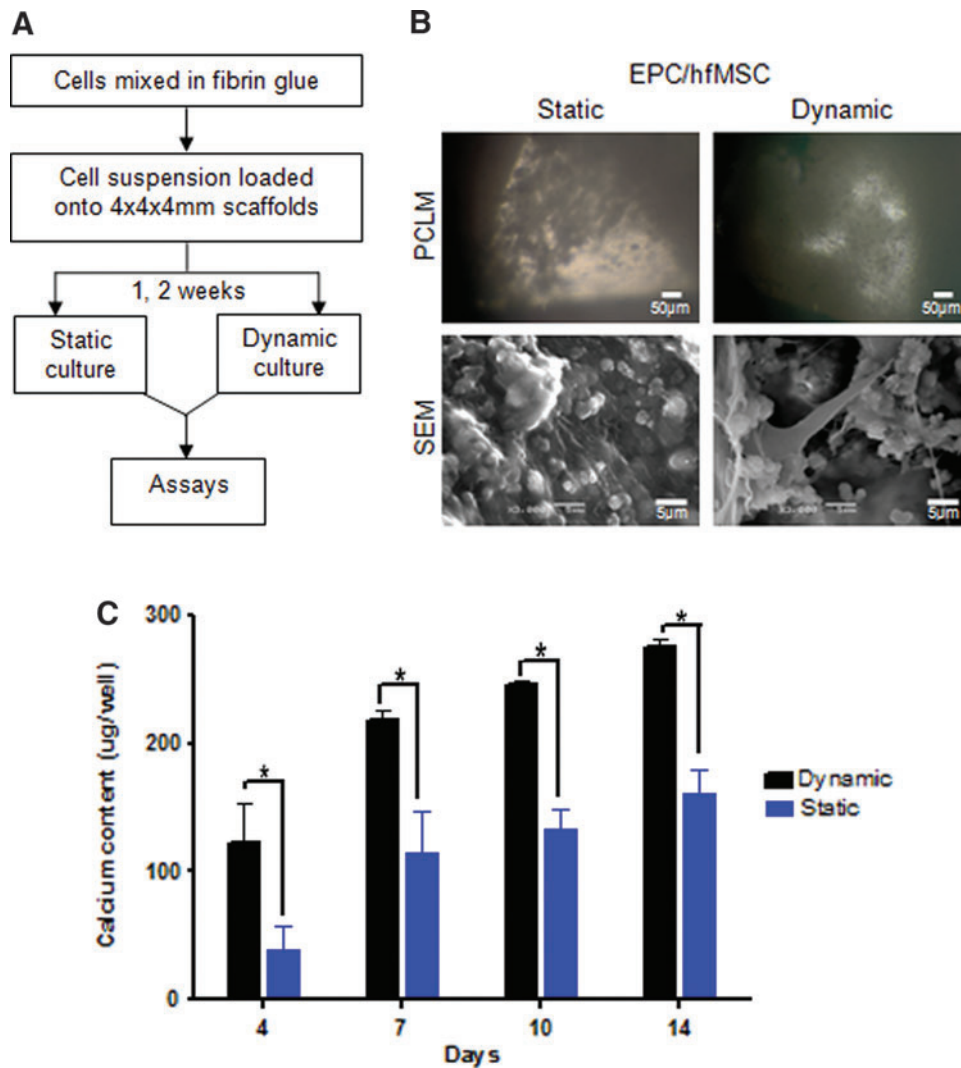
FIG. 3. Dynamic bioreactor culture of EPC/hfMSC constructs induced greater mineralization, but did not exhibit vessel-forming ability *in vitro* as compared to static culture. **(A)** Experimental workflow for comparison of EPC/hfMSC constructs in static and dynamic conditions. **(B)** Higher levels of mineralization were observed within the pores of dynamically cultured scaffolds by phase-contrast light microscopy (pCLM) on day 14. SEM also showed more prominent network of extracellular matrix formation. **(C)** Dynamically cultured constructs showed 1.7×higher levels of calcium deposited across all time points compared to static culture ($p < 0.001$). **(D)** Dual fluorescently labeled EPC/hfMSC cocultures were seen to maintain viability in both static and dynamic culture. Vessel-like networks were formed in the 3D constructs under static conditions on day 7, but not in dynamic cultures or when EPC were cultured alone. By day 14, no vessels were observed in both static and dynamic cultures. **(E, F)** An extensive *in vitro* vessel network was formed in the statically cultured EPC/hfMSC cocultures, which were observed to increase with scaffold depth on day 7. Color images available online at www.liebertpub.com/tea
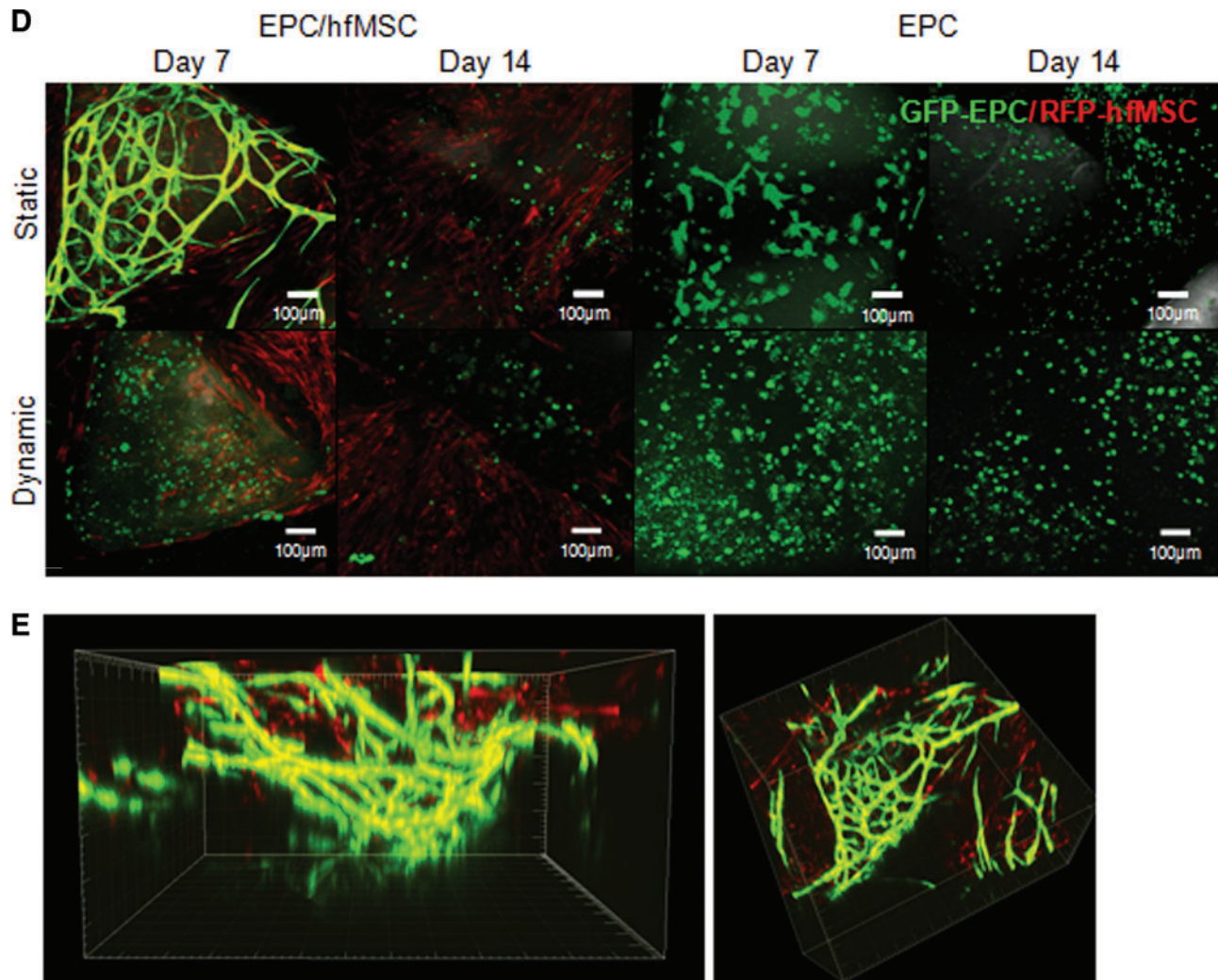
FIG. 3. (Continued).

CD34, and CD45) and were positive for CD73, CD105, and CD90.[22]

Dynamic culture of EPC/hfMSC constructs led to greater mineralization in vitro, *but did not exhibit vessel formation as compared to static culture*

We explored the effects of introducing biomechanical forces with a biaxial bioreactor (Fig. 2C, D) on EPC/hfMSC cocultured scaffolds for 2 weeks before vascularization and osteogenic differentiation assays (Fig. 3A). Phase-contrast light microscopy showed enhanced mineralization within the pores of dynamically cultured scaffolds (Fig. 3B), with more prominent trabecular-like networks of extracellular matrix formation on day 14 (SEM; Fig. 3B). Quantitatively, 1.7-fold more calcium was deposited in dynamically cultured over statically cultured scaffolds on day 14 ($p < 0.05$, Fig. 3C). Both treatment groups also maintained high degrees of cell viability over 14 days of culture as seen by the continuous expression of both fluorescent proteins (Fig. 3D). In terms of its vessel-forming ability, dynamic bioreactor culture of EPC/hfMSC was unable to induce any *in vitro* vessel formation over all 14 days. However, it was noted that EPC

were able to form vessel-like networks upon coculture with hfMSC under static conditions in the 3D microenvironment on day 7 (Fig. 3D–F and Supplementary Video S1; Supplementary Data are available online at www.liebertpub.com/tea), but the vascular network is no longer present by day 14 of culture (Fig. 3D). Hence, at the time of implantation, both dynamic and statically cultured EPC/hfMSC cocultured scaffolds had no vessel networks, although cellular viability of both EPC and hfMSC were high as shown by the continued expression of their respective fluorescent proteins. EPC alone also did not exhibit the ability to form vessel-like structures in the absence of hfMSC (Fig. 3D).

Dynamically cultured constructs exhibit earlier vasculogenesis and enhanced ectopic bone formation in vivo *compared to statically cultured constructs*

Next, we implanted all three scaffold groups (dynamic, static, and acellular) subcutaneously into immunodeficient mice to test their *in vivo* vascularization and osteogenic potential (Fig. 4A). Histological sections of MT staining exhibited larger regions of premineralizing collagen in dynamically cultured scaffolds on week 4. Capillaries, which
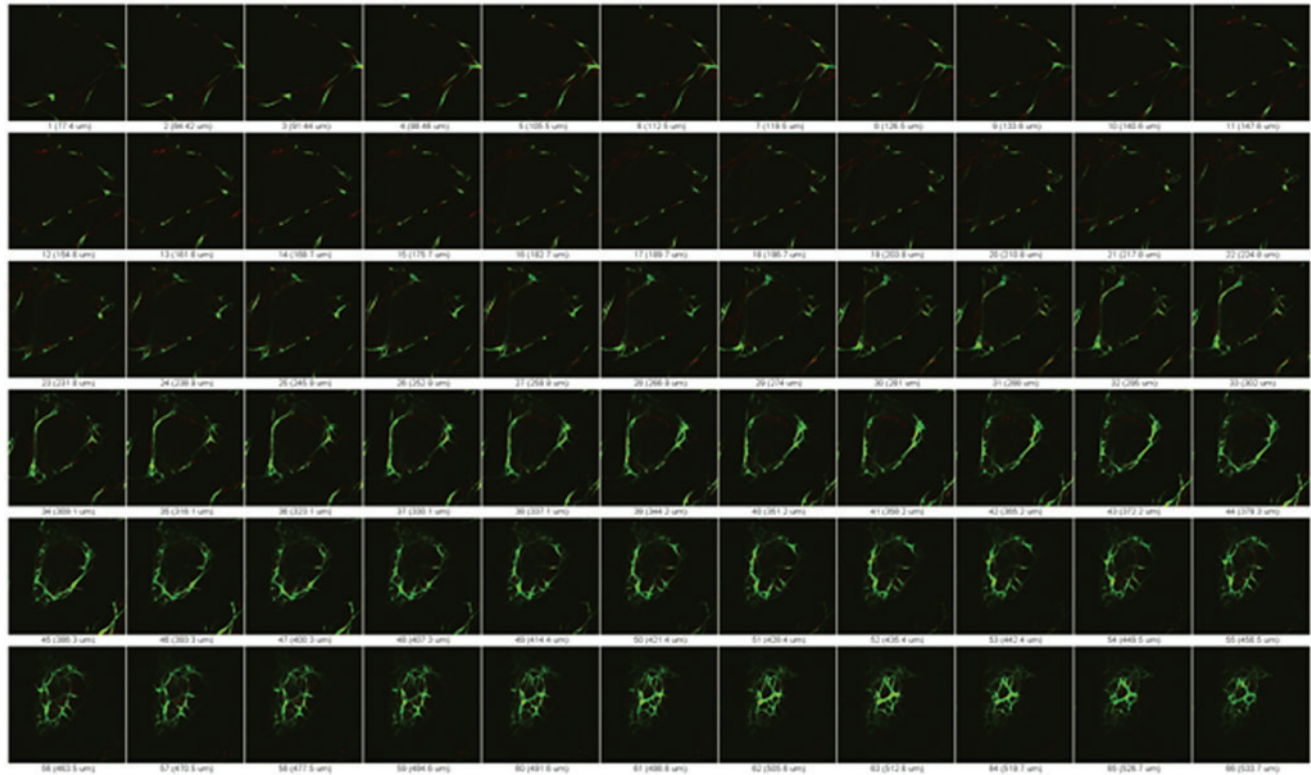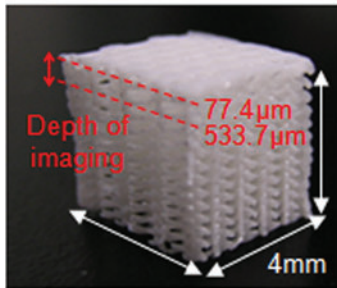
FIG. 3. (Continued).

can be seen as luminal structures filled with red blood cells, were most abundant in the dynamically cultured scaffolds, being 1.2- and 2.3-fold more numerous than the static and acellular controls, respectively ($p > 0.05$; $p < 0.01$ respectively; Fig. 4B). Cross-sectional analyses of contrast-perfused scaffolds on Micro-CT further revealed an extensive network of fine capillary structures in the central pores of dynamically cultured scaffolds as compared to fewer vessel occurrences in the static and acellular–scaffolds 8 weeks postimplantation (Fig. 4C).

Dynamically cultured scaffolds exhibited 1.4-fold higher human:mouse chimerism, which showed a more homogenous cellular distribution throughout the scaffold as compared to the statically cultured constructs, which had higher numbers of murine cells at the peripheral parts of the scaffold edges 8 weeks postimplantation ($54.6\% \pm 15.7\%$ vs. $77.7\% \pm 4.5\%$; $p < 0.001$, Fig. 4D). Dynamically cultured EPC/hfMSC scaffolds also laid down more human osteopontin at the sides of the scaffolds, with larger areas of Von Kossa staining compared with statically cultured scaffolds (week 8, Fig. 4E).

Discussion

The lack of angiogenesis in large bone grafts remains a key challenge for clinical translation for BTE, with several strategies being undertaken to prevascularize osteogenic constructs before site implantation[24] for accelerating fracture repair. Despite the growing interest in the use of coculture systems for *in vitro* prevascularization in BTE in the recent years,[10–15,24,25] and the markedly improved performance of dynamically cultured MSC-based tissue-engineered bone grafts,[17,26,27] a dynamic culture system has not been explored for optimization of coculture systems for vascularized BTE. In this study, we leveraged the osteogenic and vasculogenic potency of primitive cell sources, namely, hfMSC and EPC, respectively, cultured within a 3D dynamic system to mechanically stimulate and prime the cellular constructs. We
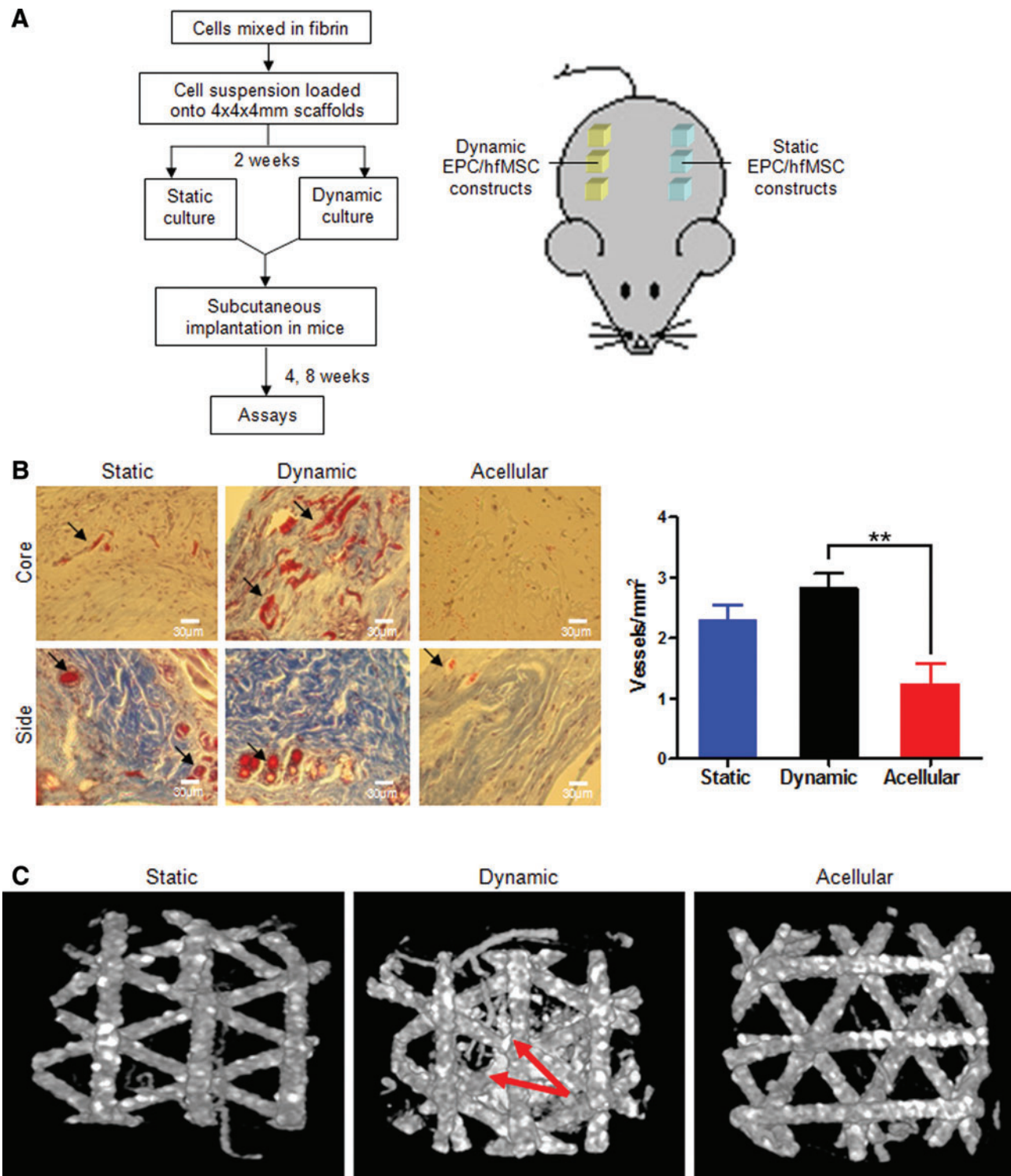
FIG. 4. Dynamic bioreactor culture induced greater vascularization, new bone formation, and maintain higher cellular viability of EPC/hfMSC constructs *in vivo* compared to static culture. **(A)** Flow-chart of the experimental workflow comparing static and dynamic bioreactor culture upon subcutaneous implantation in mice for 8 weeks. **(B)** Masson's Trichrome staining showed denser and more compact tissue formation, with greater number of capillary structures containing red blood cells (black arrows) in the core of dynamically cultured sections on week 4. Higher levels of premineralizing collagen (blue stains) with perfused luminal structures are found at the edges of the scaffold, with capillary density 1.2 and 2.3× higher than static and acellular groups, respectively ($p > 0.05$; $p < 0.01$). **(C)** Microcomputed tomography analysis of the scaffold volume showed presence of a capillary network formation within the central pores of dynamically cultured scaffolds (red arrows) as compared to static and acellular scaffolds on week 8, which showed no observable differences. **(D)** Confocal imaging of histological sections showed 1.4× ($p < 0.001$) higher human:mouse chimerism upon anti-human lamins A/C staining on week 8. **(E)** Von Kossa staining showed greater regions of ectopic mineralization (black stains indicated by white arrows; scaffolds were indicated by S) and a larger area of rabbit anti-human osteopontin staining in dynamically cultured constructs compared to static constructs on week 8. Color images available online at www.liebertpub.com/tea
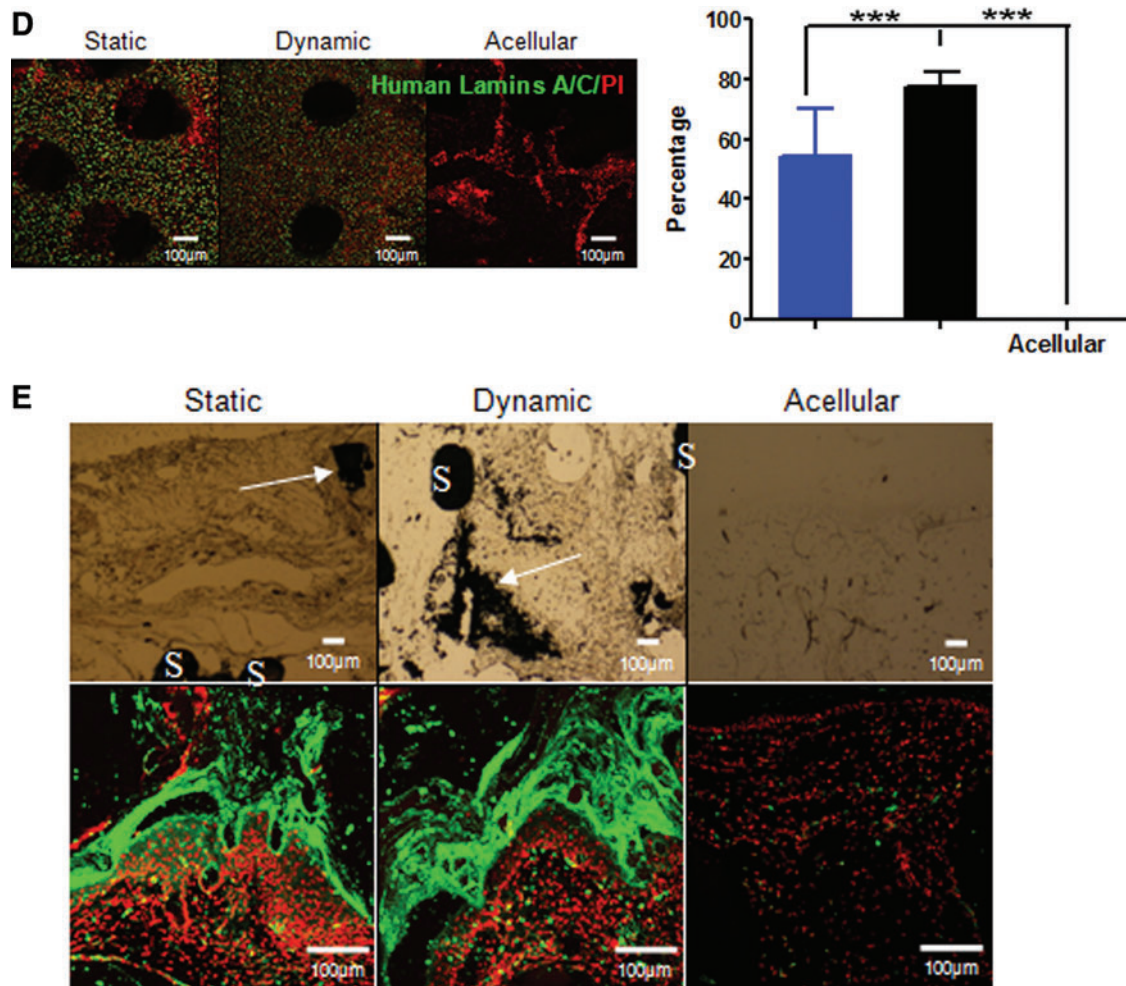
FIG. 4. (Continued).

observed improved mineralization of scaffolds *in vitro*, the laying down of more human osteopontin and formation of more compact bone *in vivo* in dynamically cultured scaffolds compared to statically cultured scaffolds. In addition, dynamically cultured scaffolds resulted in improved vascularization and a significantly higher donor cell survival postimplantation *in vivo*.

Currently, various groups have utilized the approach of *in vitro* prevascularization through a coculture of endothelial lineages and osteoblast-like cell types. Some have demonstrated enhanced neovascularization with the formation of highly organized prevascular structures upon coculture *in vitro*, which anastomosized and integrated with host blood vessels *in vivo* as compared to the use of singular cell sources.[12,22,25] Only a few groups have reported an accompanied improvement in bone formation.[13,14,22] Usami *et al.* showed a 1.6-fold increase in capillary density and a slight increase by 1.3-fold in bone formation in canine-EPC/MSC compared to MSC alone[14]; Orthotopic implantation of the EPC/MSC construct led to earlier vascularization and significantly more bone formation in a critical-sized femoral defect rat model, with higher ultimate loading than the MSC-alone group.[13] In contrast, Koob *et al.* showed no improvement in bone formation upon coculture of human umbilical vein endothelial

cells (HUVEC) with MSC, despite a higher neovessel formation in HUVEC/MSC spheroids in a critical-sized mouse calvarial defect,[28] while Geuze *et al.* showed that goat-EPC/MSC did not have a higher bone content compared to MSC alone upon ectopic implantation in a goat model.[29] This poor correlation of vessel formation and inconsistent functional contributions toward aiding bone formation could possibly be influenced by the use of functionally different species-specific cell types/sources. In addition, the lack of biomechanical stimulation is likely necessary for osteogenic maturation and functional vessel network formation,[30] which require further experiments for verification.

To date, there had been no investigations into the efficacy of a dynamic culture in coculture systems for the purpose of improving vascularization and bone formation as compared to a static environment for vascularized BTE. Grellier and coworkers are thus far, the only team that utilized a dynamic culture for the culture of cell-encapsulated alginate microspheres in a spinner flask before assaying or implantation,[15] investigating cellular metabolic activity and osteogenic gene expression of its cocultures of human osteoprogenitors and HUVEC to its monocultures. However, there was no comparison made with a 3D static environment to demonstrate its contributions toward both vasculogenic and osteogenic

efficacy. Dynamic culture conditions may expose endothelial cells to the physiological shear forces, which control many aspects governing the fate of endothelial cells, such as the mediation of transcriptional changes, endothelial sprouting,[31] proliferation,[32] and vessel homeostasis.[33,34] Indeed, dynamic culture conditions have already been demonstrated to be advantageous in BTE, with our group and many others demonstrating profound improvements in cellular viability and bone formation in dynamically cultured scaffolds.[17,35]

In our biaxial bioreactor culture, we observed consistently a higher calcium deposition across all 14 days of *in vitro* culture, with a more prominent extracellular matrix formation. While both dynamic and static culture demonstrated a high level of cellular viability *in vitro*, dynamically cultured constructs exhibited higher human:mouse chimerism over statically cultured EPC/hfMSC-scaffolds 8-weeks postimplantation. The higher degree of human cell chimerism distributed homogenously throughout the core of dynamically cultured scaffolds suggests the rapid establishment of a vascular blood supply upon implantation. Mechanical stimulation of the bioreactor could have induced greater EPC viability, hence, promoting vessel formation in the dyamically culture scaffolds *in vivo*. This is particularly important in larger grafts where poor mass transport is poor toward the central core of the scaffold. In agreement with our previous work with hfMSC-scaffolds, Zhang *et al.* demonstrated the ability of dynamic culture in sustaining cellular viability after 28 days of dynamic culture, avoiding massive necrosis seen in statically cultured scaffolds loaded with hfMSC.[17]

The inability to form a vessel network within the dynamically cultured constructs as compared to the extensive vessel network formation under static conditions was unexpected, although we speculate that the increased mass transport in the bioreactor may have reduced the potent hypoxic gradient in the core of the scaffold. As theoretically modeled by Muschler *et al.*,[36] an oxygen gradient from the scaffold centre to the surface is created based on a balance between cellular density, their oxygen consumption, as well as diffusion distance within the scaffold. Experimentally, Volkmer *et al.* demonstrated a central hypoxic gradient in 3D scaffolds, which had a corresponding effect on cellular viability.[37] Furthermore, it has been well documented that angiogenesis is driven by hypoxia,[38] which directs endothelial tip cells to migrate toward the direction of low oxygen tensions, and initiates capillary outgrowths.[39] In addition, the transient generation of a complex vascular network under static conditions *in vitro* could have been influenced by suboptimal culture conditions, leading on to poor EPC survival. In agreement with our previous study, we showed a high level of EPC confluence at day 7 of both dynamic and static cultures, which subsequently declined in cell numbers by day 14 of BM culture.[22] Due to the complexity of coculture systems and the different requirements of each cell type governing cellular behavior and differentiation, the choice of optimal culture conditions remains a challenge.[40,41]

Although dynamic bioreactor culture could not induce *in vitro* vessel formation, subsequent implantation *in vivo* demonstrated earlier initiation of neovasculogenesis upon dynamic culture, where a higher capillary density was noted as well as a fine capillary network existing within the central pores of the dynamically cultured scaffolds over 8 weeks postimplantation. This result suggests the rapid formation of vessels, possibly mediated by the secretion of vasoactive cytokines upon biomechanical stimulation as well as a higher cellular viability observed 8 weeks postimplantation. This, in turn, could have assisted in the formation of a greater ectopic bone formation. Alternatively, direct mechanostimulatory contributions exerted by biomechanical stresses onto the cells could have triggered the induction of vasculogenesis[42,43] and enhanced osteogenic differentiation of MSC.[44] Here, we verified our previous *in vivo* data on the efficacy of biaxial bioreactor priming for the osteogenic maturation of BTE constructs,[16,17] but also highlight its ability to induce earlier vasculogenesis in the EPC/hfMSC constructs.

Conclusion

Angiogenesis plays a critical role in aiding bone formation and accelerating fracture repair. Current studies using coculture systems have failed to show maturity of vessel and bone formation possibly due to the lack of biomechanical stimulation onto coculture constructs. Using an integrated approach of bioresorbable polymeric scaffold and bioreactor technologies, we demonstrated the efficacy of a EPC/hfMSC coculture system on prevascularizing a bone graft under dynamic conditions with early initiation of neovasculogenesis of EPC/hfMSC construct upon mechanical stimuli from the biaxial motion of the bioreactor. Future work will investigate the influence of oxygen tension in establishing the vascular network *in vitro* as well as optimize the time of exposure to dynamic bioreactor culture before implantation to derive the maximal response in vessel formation and osteogenic regeneration. Successful demonstration of vascularization and accelerated bony repair in a large orthotopic animal model in future studies will present viable options for the treatment of large bony defects in the clinical realm.

Disclosure Statement

No competing financial interests exist.

References

1. Kanczler, J.M., and Oreffo, R.O. Osteogenesis and angiogenesis: the potential for engineering bone. Eur Cell Mater **15,** 100, 2008.
2. Ko, H.C., Milthorpe, B.K., and McFarland, C.D. Engineering thick tissues—the vascularisation problem. Eur Cell Mater **14,** 1; discussion 9, 2007.
3. Vacanti, C.A., Bonassar, L.J., Vacanti, M.P., and Shufflebarger, J. Replacement of an avulsed phalanx with tissue-engineered bone. N Engl J Med **344,** 1511, 2001.

4. Quarto, R., Mastrogiacomo, M., Cancedda, R., Kutepov, S.M., Mukhachev, V., Lavroukov, A., et al. Repair of large bone defects with the use of autologous bone marrow stromal cells. N Engl J Med 344, 385, 2001.

5. Schimming, R., and Schmelzeisen, R. Tissue-engineered bone for maxillary sinus augmentation. J Oral Maxillofac Surg 62, 724, 2004.

6. Marcacci, M., Kon, E., Moukhachev, V., Lavroukov, A., Kutepov, S., Quarto, R., et al. Stem cells associated with macroporous bioceramics for long bone repair: 6- to 7-year outcome of a pilot clinical study. Tissue Eng 13, 947, 2007.

7. Cancedda, R., Giannoni, P., and Mastrogiacomo, M. A tissue engineering approach to bone repair in large animal models and in clinical practice. Biomaterials 28, 4240, 2007.

8. Zhang, Z.Y., Teoh, S.H., Chong, M.S., Lee, E.S., Tan, L.G., Mattar, C.N., et al. Neo-vascularization and bone formation mediated by fetal mesenchymal stem cell tissue-engineered bone grafts in critical-size femoral defects. Biomaterials 31, 608, 2010.

9. Zhang, Z.Y., Teoh, S.H., Hui, J.H., Fisk, N.M., Choolani, M., and Chan, J.K. The potential of human fetal mesenchymal stem cells for off-the-shelf bone tissue engineering application. Biomaterials 33, 2656, 2012.

10. Unger, R.E., Ghanaati, S., Orth, C., Sartoris, A., Barbeck, M., Halstenberg, S., et al. The rapid anastomosis between prevascularized networks on silk fibroin scaffolds generated in vitro with cocultures of human microvascular endothelial and osteoblast cells and the host vasculature. Biomaterials 31, 6959, 2010.

11. Melero-Martin, J.M., De Obaldia, M.E., Kang, S.Y., Khan, Z.A., Yuan, L., Oettgen, P., et al. Engineering robust and functional vascular networks in vivo with human adult and cord blood-derived progenitor cells. Circ Res 103, 194, 2008.

12. Tsigkou, O., Pomerantseva, I., Spencer, J.A., Redondo, P.A., Hart, A.R., O'Doherty, E., et al. Engineered vascularized bone grafts. Proc Natl Acad Sci U S A 107, 3311, 2010.

13. Seebach, C., Henrich, D., Kahling, C., Wilhelm, K., Tami, A.E., Alini, M., et al. Endothelial progenitor cells and mesenchymal stem cells seeded onto beta-TCP granules enhance early vascularization and bone healing in a critical-sized bone defect in rats. Tissue Eng Part A 16, 1961, 2010.

14. Usami, K., Mizuno, H., Okada, K., Narita, Y., Aoki, M., Kondo, T., et al. Composite implantation of mesenchymal stem cells with endothelial progenitor cells enhances tissue-engineered bone formation. J Biomed Mater Res A 90, 730, 2009.

15. Grellier, M., Granja, P.L., Fricain, J.C., Bidarra, S.J., Renard, M., Bareille, R., et al. The effect of the co-immobilization of human osteoprogenitors and endothelial cells within alginate microspheres on mineralization in a bone defect. Biomaterials 30, 3271, 2009.

16. Zhang, Z.Y., Teoh, S.H., Teo, E.Y., Khoon Chong, M.S., Shin, C.W., Tien, F.T., et al. A comparison of bioreactors for culture of fetal mesenchymal stem cells for bone tissue engineering. Biomaterials 31, 8684, 2010.

17. Zhang, Z.Y., Teoh, S.H., Chong, W.S., Foo, T.T., Chng, Y.C., Choolani, M., et al. A biaxial rotating bioreactor for the culture of fetal mesenchymal stem cells for bone tissue engineering. Biomaterials 30, 2694, 2009.

18. Zhang, Z.Y., Teoh, S.H., Chong, M.S., Schantz, J.T., Fisk, N.M., Choolani, M.A., et al. Superior osteogenic capacity for bone tissue engineering of fetal compared to perinatal and adult mesenchymal stem cells. Stem Cells 27, 126, 2009.

19. Murohara, T. Cord blood-derived early outgrowth endothelial progenitor cells. Microvasc Res 79, 174, 2010.

20. Chong, M.S., and Chan, J. Lentiviral vector transduction of fetal mesenchymal stem cells. Methods Mol Biol 614, 135, 2010.

21. Chong, M.S., Chan, J., Choolani, M., Lee, C.N., and Teoh, S.H. Development of cell-selective films for layered co-culturing of vascular progenitor cells. Biomaterials 30, 2241, 2009.

22. Liu, Y., Teoh, S.H., Chong, M.S., Lee, E.S., Mattar, C.N., Randhawa, N.K., et al. Vasculogenic and osteogenesis-enhancing potential of human umbilical cord blood endothelial colony-forming cells. Stem Cells 30, 1911, 2012.

23. Bolland, B.J., Kanczler, J.M., Dunlop, D.G., and Oreffo, R.O. Development of in vivo muCT evaluation of neovascularisation in tissue engineered bone constructs. Bone 43, 195, 2008.

24. Rouwkema, J., Rivron, N.C., and van Blitterswijk, C.A. Vascularization in tissue engineering. Trends Biotechnol 26, 434, 2008.

25. Fuchs, S., Ghanaati, S., Orth, C., Barbeck, M., Kolbe, M., Hofmann, A., et al. Contribution of outgrowth endothelial cells from human peripheral blood on in vivo vascularization of bone tissue engineered constructs based on starch polycaprolactone scaffolds. Biomaterials 30, 526, 2009.

26. Kreke, M.R., Sharp, L.A., Lee, Y.W., and Goldstein, A.S. Effect of intermittent shear stress on mechanotransductive signaling and osteoblastic differentiation of bone marrow stromal cells. Tissue Eng Part A 14, 529, 2008.

27. Sikavitsas, V.I., Bancroft, G.N., Lemoine, J.J., Liebschner, M.A., Dauner, M., and Mikos, A.G. Flow perfusion enhances the calcified matrix deposition of marrow stromal cells in biodegradable nonwoven fiber mesh scaffolds. Ann Biomed Eng 33, 63, 2005.

28. Koob, S., Torio-Padron, N., Stark, G.B., Hannig, C., Stankovic, Z., and Finkenzeller, G. Bone formation and neovascularization mediated by mesenchymal stem cells and endothelial cells in critical-sized calvarial defects. Tissue Eng Part A 17, 311, 2011.

29. Geuze, R.E., Wegman, F., Oner, F.C., Dhert, W.J., and Alblas, J. Influence of endothelial progenitor cells and platelet gel on tissue-engineered bone ectopically in goats. Tissue Eng Part A 15, 3669, 2009.

30. Stolberg, S., and McCloskey, K.E. Can shear stress direct stem cell fate? Biotechnol Prog 25, 10, 2009.

31. Song, J.W., and Munn, L.L. Fluid forces control endothelial sprouting. Proc Natl Acad Sci U S A 108, 15342, 2011.

32. Lin, K., Hsu, P.P., Chen, B.P., Yuan, S., Usami, S., Shyy, J.Y., et al. Molecular mechanism of endothelial growth arrest by laminar shear stress. Proc Natl Acad Sci U S A 97, 9385, 2000.

33. Hudlicka, O., Brown, M.D., May, S., Zakrzewicz, A., and Pries, A.R. Changes in capillary shear stress in skeletal muscles exposed to long-term activity: role of nitric oxide. Microcirculation 13, 249, 2006.

34. Jones, E.A., le Noble, F., and Eichmann, A. What determines blood vessel structure? Genetic prespecification vs. hemodynamics. Physiology (Bethesda) 21, 388, 2006.

35. McCoy, R.J., and O'Brien, F.J. Influence of shear stress in perfusion bioreactor cultures for the development of three-dimensional bone tissue constructs: a review. Tissue Eng Part B Rev 16, 587, 2010.

36. Muschler, G.F., Nakamoto, C., and Griffith, L.G. Engineering principles of clinical cell-based tissue engineering. J Bone Joint Surg Am 86-A, 1541, 2004.

37. Volkmer, E., Drosse, I., Otto, S., Stangelmayer, A., Stengele, M., Kallukalam, B.C., *et al.* Hypoxia in static and dynamic 3D culture systems for tissue engineering of bone. Tissue Eng Part A **14,** 1331, 2008.

38. Coulon, C., Georgiadou, M., Roncal, C., De Bock, K., Langenberg, T., and Carmeliet, P. From vessel sprouting to normalization: role of the prolyl hydroxylase domain protein/hypoxia-inducible factor oxygen-sensing machinery. Arterioscler Thromb Vasc Biol **30,** 2331, 2010.

39. Germain, S., Monnot, C., Muller, L., and Eichmann, A. Hypoxia-driven angiogenesis: role of tip cells and extracellular matrix scaffolding. Curr Opin Hematol **17,** 245, 2010.

40. Liu, Y., Chan, J., and Teoh, S.H. Review on vascularised bone tissue engineering strategies: focus on coculture systems J Tissue Eng Regen Med, 2012. DOI: 10.1002/term.1617. http://onlinelibrary.wiley.com/doi/10.1002/term.1617/abstract;jsessionid=8E36DEF693D1476CBDCBD147FD128000.d03t01

41. Kirkpatrick, C.J., Fuchs, S., and Unger, R.E. Co-culture systems for vascularization—learning from nature. Adv Drug Deliv Rev **63,** 291, 2011.

42. Yamamoto, K., Takahashi, T., Asahara, T., Ohura, N., Sokabe, T., Kamiya, A., *et al.* Proliferation, differentiation, and tube formation by endothelial progenitor cells in response to shear stress. J Appl Physiol **95,** 2081, 2003.

43. Yamamoto, K., Sokabe, T., Watabe, T., Miyazono, K., Yamashita, J.K., Obi, S., *et al.* Fluid shear stress induces differentiation of Flk-1-positive embryonic stem cells into vascular endothelial cells *in vitro*. Am J Physiol Heart Circ Physiol **288,** H1915, 2005.

44. Kimelman-Bleich, N., Seliktar, D., Kallai, I., Helm, G.A., Gazit, Z., Gazit, D., *et al.* The effect of *ex vivo* dynamic loading on the osteogenic differentiation of genetically engineered mesenchymal stem cell model. J Tissue Eng Regen Med **5,** 384, 2011.

Address correspondence to:
Jerry K.Y. Chan, MRCOG, PhD
Experimental Fetal Medicine Group
Department of Obstetrics and Gynaecology
Yong Loo Lin School of Medicine
National University of Singapore
1E Kent Ridge Road
Singapore 119228

E-mail: jerrychan@nus.edu.sg

Swee-Hin Teoh, PhD
Division of Bioengineering
School of Chemical and Biomedical Engineering
Nanyang Technological University
70 Nanyang Drive
Singapore 637457

E-mail: teohsh@ntu.edu.sg